Journal of Thermal Analysis and Calorimetry (2021) 144:525–538
https://doi.org/10.1007/s10973-020-10368-9

Study on preparation and properties of agricultural waste bagasse eco-type bio-flame-retardant/epoxy composites

Ming-Yuan Shen[1] · Chen-Feng Kuan[2] · Hsu-Chiang Kuan[2] · Cing-Yu Ke[3] · Chin-Lung Chiang[3]

Received: 30 April 2020 / Accepted: 15 October 2020 / Published online: 27 November 2020

Abstract

We used agricultural waste bagasse as a flame retardant to improve the flammability problem of epoxy. A ring-opening reaction was conducted on the hydroxyl group of bagasse and the epoxy of triglycidyl isocyanurate (TGIC) to form TGIC-bagasse. Subsequently, 9,10-dihydro-9-oxa-10-phosphaphenanthrene-10-oxide (DOPO) was incorporated, and the active hydrogen of DOPO reacted with the epoxy group of TGIC to form bagasse@TGIC@DOPO, and this flame retardant was introduced to the epoxy matrix to prepare a composite material with an interpenetrating network (IPN) structure. Fourier-transform infrared spectroscopy (FT-IR), thermogravimetric analyzer (TGA), the limiting oxygen index (LOI), the UL-94, thermal analysis-FT-IR (TA-FTIR), and X-ray photoelectron spectroscopy were used to identify structural, thermal, and flame-retardant properties and toxicity and char analysis. The TGA results revealed that the char yield increased from 14.1 mass% of epoxy to 23.4 mass% after bagasse@TGIC@DOPO was added, thereby improving the thermal stability of compound materials. The LOI and UL-94 indicated that after adding, the LOI and UL-94 improved from 21 (fail) to 29 (V-0). These results revealed that epoxy/bagasse@TGIC@DOPO IPN composite material had a strong flame-retardant effect.

Keywords Agricultural waste product · Bagasse · Epoxy · Flame retardant · Interpenetrating polymer network

Introduction

With technological advancement in recent years, the need for polymeric material materials has grown. Polymers are nearly everywhere in our lives. However, fires in public places or at home may result in casualties and property losses. Fires in general fireproof buildings occur in five stages: the incipient, growth, flashover, fully developed, and decay stages. The time from when a fire begins to burn until flashover occurs is the flashover time, the length of which affects whether individuals inside the building can successfully escape from a fire and the difficulty of rescue by firefighters. Once a flashover occurs inside a building, all combustible materials burn fully, and indoor temperatures rise from 200–300 to 800–1200 °C. Consequently, individuals have an extremely slim chance of surviving in spaces where a flashover occurs. Therefore, delaying or preventing flashover or enabling firefighters to conduct various emergency responses before flashover occurs is crucial to fire prevention strategy. Using flame retardants can delay flashover time to achieve this goal.

Epoxy resin is a commonly used thermosetting polymer and is crucial in various industrial fields. For example, epoxy is used in coatings, paints, adhesives, insulating materials, aviation, and electronic equipment. Epoxy has excellent adhesion, chemical resistance, low shrinkage rate, and superior electrical insulation. However, epoxy is easily flammable and can produce a considerable amount of toxic gas. Thus, epoxy is a fire hazard, and its application in the fire retardance field is limited, particularly in aviation, electrical, and electronic industries. Increasingly rigorous examinations have been conducted on flame retardants because of their potential health and environmental hazards. Therefore, developing environment-friendly and halogen-free flame retardants applicable to epoxy is necessary [1–6].

✉ Chin-Lung Chiang
dragon@sunrise.hk.edu.tw

[1] Department of Mechanical Engineering, National Chin-Yi University of Technology, Taichung 411, Taiwan

[2] Department of Food Beverage Management, Far East University, Tainan 744, Taiwan

[3] Green Flame Retardant Material Research LaboratoryDepartment of Safety, Health and Environmental Engineering, Hung-Kuang University, Taichung 433, Taiwan

Flame retardants containing halogen are widely used in polymer materials to effectively improve flame retardancy. However, some flame retardants such as polybrominated diphenyl ethers (PBDEs) and polybrominated biphenyl (PBB) release a considerable amount of toxic and corrosive gases during combustion that produces persistent environmental and ecological pollution and causes bioaccumulation. Consequently, adding these harmful substances to polymer materials is prohibited [7, 8]. The Waste electrical and electronic equipment directive (WEEE) aims to prevent or reduce the adverse effects of producing electrical and electronic equipment and handling waste products, reduce the overall impact of resource consumption, and increase the efficiency of such consumption to protect the environment and human health, thereby contributing to sustainable development [9]. The restriction of hazardous substances directive (RoHS) has elaborated on the WEEE by prohibiting electronic and electrical equipment that contains Pb, Cd, Hg, Cr^{+6}, PBB, and PBDE since July 1, 2006. However, on June 8, 2011, four substances—hexabromocyclododecane, di(2-ethylhexyl) phthalate, benzyl butyl phthalate, and dibutyl phthalate—were proposed and prioritized in the prohibition because they pose risks to human health and the environment [10, 11].

For environmental protection, green and environmentally friendly composite materials (e.g., agricultural waste products including straw, rice husk, and bagasse) are promoted around the world. Bagasse is an easily obtainable agricultural waste product and can enhance mechanical and physical properties, reduce flammability during combustion, and reduce the amount of artificial flame retardants used. Therefore, bio-composite materials have academic value and can be applied in fields including optics, electronics, energy, smart coatings, fuels, flame retardants, and composite materials [12–14].

Therefore, we used agricultural waste reuse and green halogen-free concepts to prepare flame retardants that contain nitrogen and phosphorus and blend them into epoxy resin to create flame-retardant composite materials and improve their thermal properties and flame retardancy of polymer substrates [2, 15–17]. These materials can be used in transportation, coating, composite, and building materials, and thereby widening polymer applications.

Experimental

Materials

DGEBA-type epoxy was kindly supplied by Nan-Ya Plastics Corporation, Taipei City, Taiwan. 4,4′-Diaminodiphenylmethane (DDM) as a curing agent for epoxy and 9,10-dihydro-9-oxa-10-phosphaphenanthrene-10-oxide (DOPO) were purchased from Sigma-Aldrich Co. Ltd, Irvine, UK. Bagasse was obtained from the local market. The size of the bagasse after being pulverized is 0.053 mm. Isocyanurate (TGIC) was purchased from TCI, Tokyo, Japan. Anhydrous stabilized tetrahydrofuran (THF) was obtained from Lancaster Co., Morecambe, Lancashire, UK.

Preparation of epoxy/bagasse@TGIC@DOPO IPN

First, we pulverized the bagasse, washed it with deionized water at 100 °C 3×, filtered it 3×, and put it in an oven to remove the water at 100 °C. We put bagasse (1.366 g) and triglycidyl isocyanurate (TGIC; 1.67 g) into a 100 ml serum bottle and added 80 ml of tetrahydrofuran solvent for modification and reaction at 60 °C for 2 h. This is solution A, as presented in Scheme 1. We put 9,10-dihydro-9-oxa-10-phosphaphenanthrene-10-oxide (DOPO; 2.428 g) into solution A and reacted this at 60 °C for 2 h to obtain a bagasse@TGIC@DOPO flame retardant, which is solution B, as displayed in Scheme 2. Solution B was poured into the epoxy matrix (10 g), stirred at 60 °C for 2 h before hardener 4,4′-diaminodiphenylmethane (2.75 g) was added, and observed whether viscosity increased, after which it was poured into a mold, placed at room temperature for 24 h, and placed in an oven at 60 °C. The temperature increased from 20 to 180 °C to form the composite materials as illustrated in Scheme 3.

Measurements

The FTIR spectra of the materials were recorded between 4000 and 400 cm^{-1} using a Nicolet Avatar 320 FT-IR spectrometer, from the USA. Thin films were prepared by the solution casting method. The samples were treated at 180 °C for 2 h and then ground into a fine powder. The thermal degradation of the composite was examined using a thermogravimetric analyzer (TGA) (Perkin Elmer TGA 7) from room temperature to 800 °C at a rate of 10 °C min^{-1} under an atmosphere of nitrogen. The measurements were made on 6–10 mg samples. Mass-loss/temperature curves were plotted. The degraded products were analyzed by TGA/FT-IR (209 F3/BRUKER Tensor II) from room temperature to 800 °C at a rate of 10 °C min^{-1} under an atmosphere of air. The LOI is defined as the minimum fraction of O_2 in a mixture of O_2 and N_2 that will just support flaming combustion. The LOI test was performed according to the testing procedure of the ASTM D 2836 Oxygen Index Method, with a test specimen bar 7–15 cm long, 6.5 ± 0.5 mm wide, and 3.0 ± 0.5 mm thick. The sample bars were suspended vertically and ignited by a Bunsen burner. The flame was removed and the timer was started. The concentration of oxygen was increased if the flame on the specimen was extinguished before burning for 3 min or burning away 5 cm of the bar. The oxygen content was adjusted until the limiting

Scheme 1 Reaction process of bagasse@TGIC

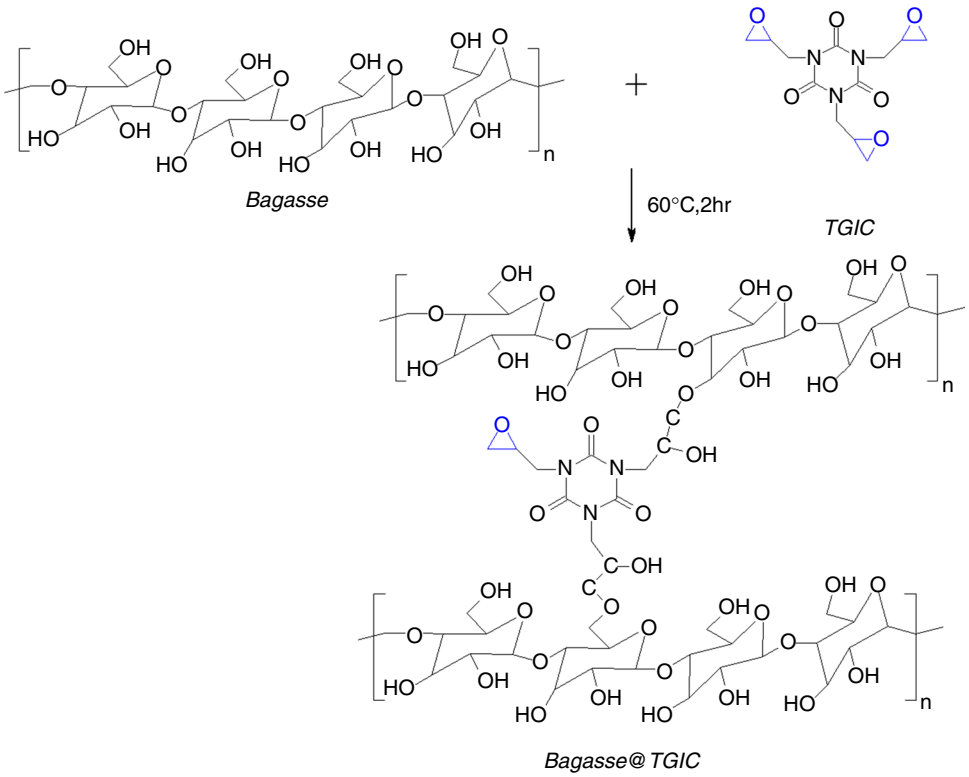

Scheme 2 Reaction process of bagasse@TGIC@DOPO

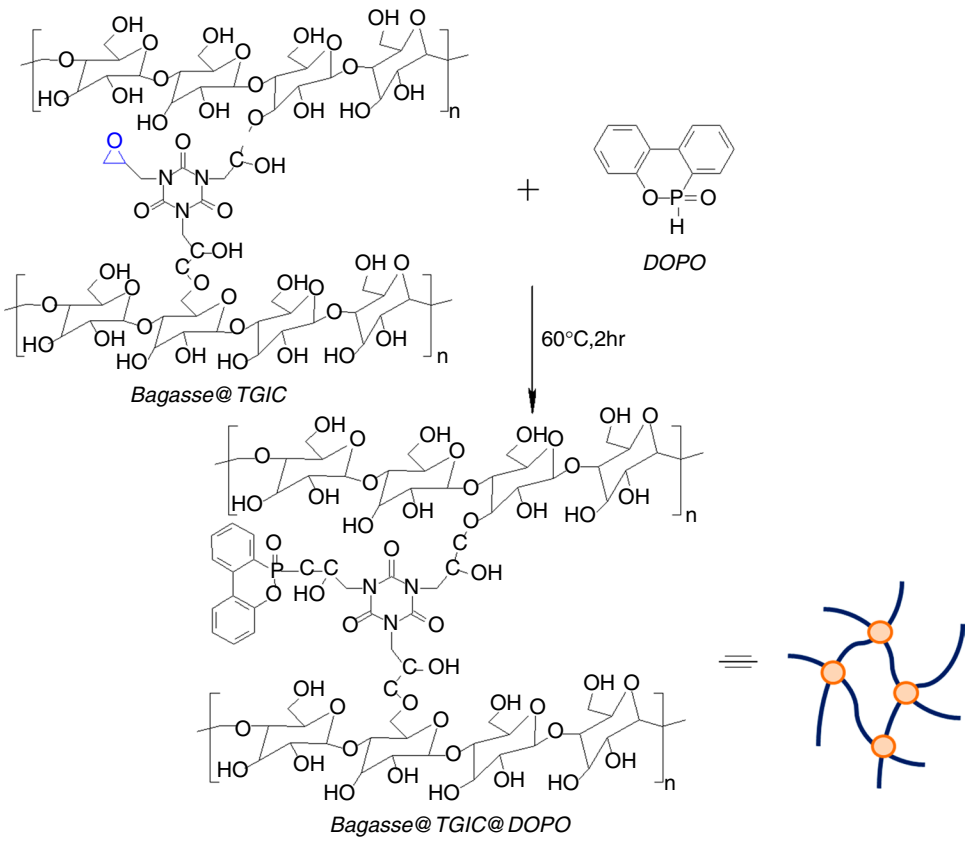

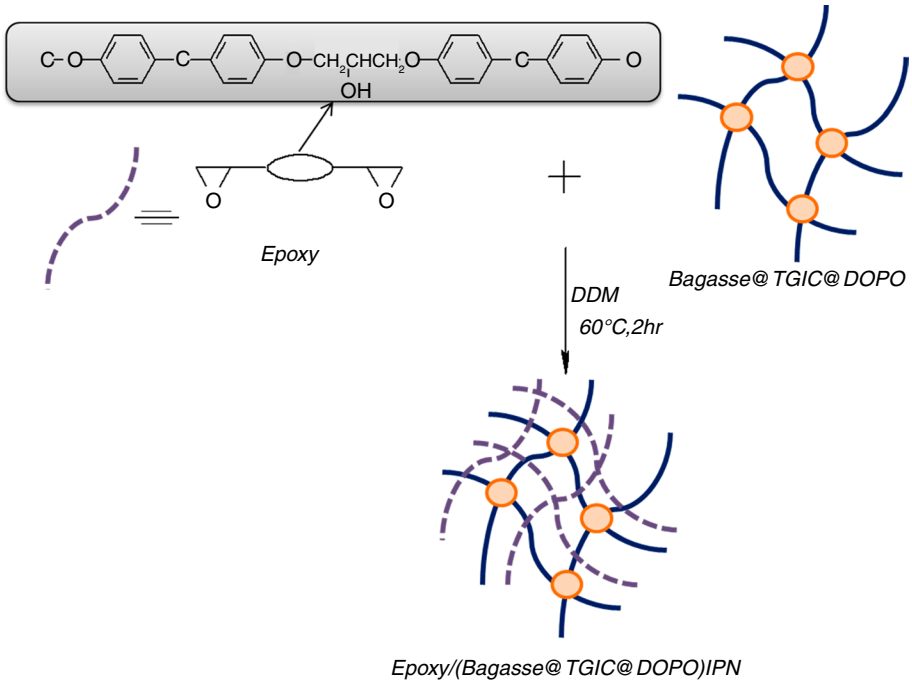

Scheme 3 Reaction process of epoxy/bagasse@TGIC@DOPO IPN

concentration was determined. The vertical burning test was done inside a fume hood. Samples were held vertically with tongs at one end and burned from the free end. Samples were exposed to an ignition source for 10 s then they were allowed to burn above cotton wool until both sample and cotton wool extinguished. Observable parameters were recorded to assess fire retardancy. The UL 94 test classifies the materials as V-0, V-1, and V-2 according to the time period needed before self-extinction and the occurrence of flaming dripping after removing the ignition source. V-0 is the most ambitious and desired classification. High-resolution X-ray photoelectron spectrometer (HR-XPS, ULVAC-PHI, Inc., Kanagawa-ken, Japan): The sample is crushed into powder, and the sample is then adhered to the aluminum sheet with small round holes, which is mainly used for detecting the sample surface as well as the element composition and distribution in vertical directions, in addition to implementing analysis on the links of element substances. The morphology of the fractured surface of the composites was studied under a scanning electron microscope (SEM) (JEOL JSM 840A, Japan). The distributions of Si atoms in the char were obtained from SEM EDX mapping (JEOL JSM 840A, Japan).

Results and discussion

Fourier-transform infrared spectroscopy

Figure 1 indicates that the characteristic absorption peak of the –OH functional group of bagasse is 3600–3200 cm^{-1} [18, 19], and the characteristic absorption peak of the TGIC epoxy group was 910 cm^{-1} [20, 21]. After a ring-opening reaction between the two, the P–H functional group of the DOPO characteristic absorption peak was at 2435 cm^{-1} [22], and the ring-opening reaction was conducted on the remaining epoxy group. Furthermore, the characteristic absorption peaks of the original bagasse, DOPO, and TGIC were observed in the bagasse@TGIC@DOPO flame retardant. We discovered that the epoxy group of TGIC and the P–H functional group of DOPO disappeared. This verified that the three successfully formed a bagasse@TGIC@DOPO flame retardant [23].

Theoretical and experimental values [24–26]

To investigate the interaction between the epoxy and DOPO-TGIC-bagasse flame retardant and the polymer matrix during thermal degradation, their calculated or theoretical value, W_c, (epoxy/bagasse@TGIC@DOPO interpenetrating polymer network (IPN) composite material) is described as follows:

$$W_c = \chi_1 \times W_1 + \chi_2 \times W_2 \quad (1)$$

where χ_1 and χ_2 are the ratios of epoxy to bagasse@TGIC@DOPO in the composite materials, respectively; and W_1 and W_2 are the independent epoxy and bagasse@TGIC@DOPO mass loss from degradation under the same conditions, respectively.

The calculated and experimental thermogravimetric analyzer (TGA) curves are displayed in Fig. 2 and Table 1. The results suggested that the calculated TGA curve was

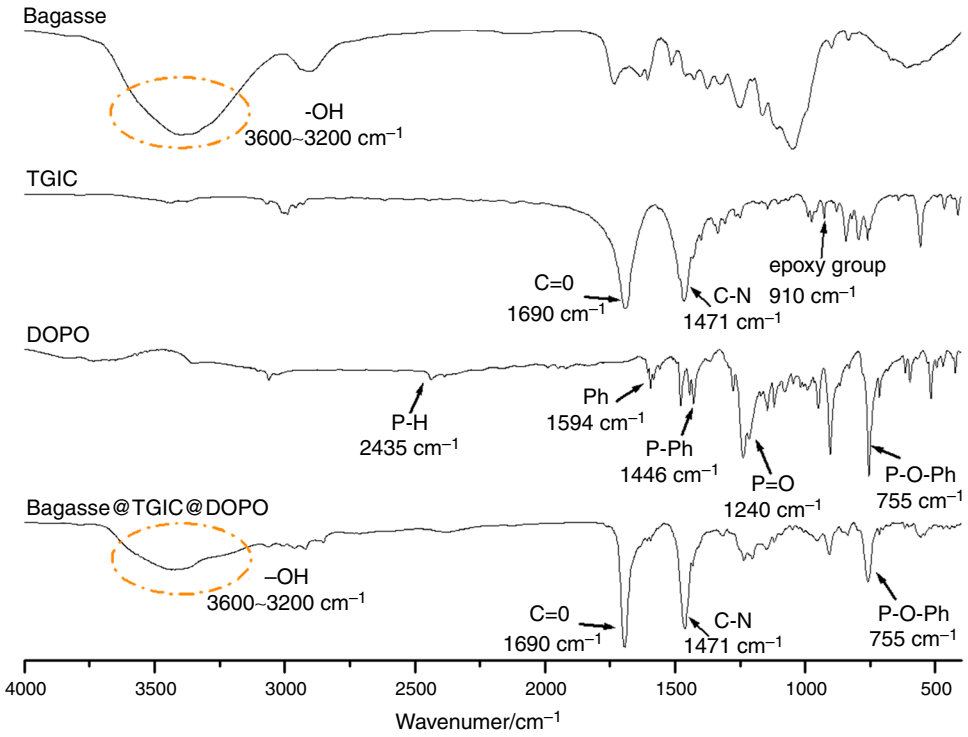

Fig. 1 FT-IR spectra of Bagasse、TGIC、DOPO and bagasse@TGIC@DOPO

lower than the experimental TGA curve. When the additive amount was between 5% and 30%, the experimental TGA curve of char yield was higher than that of the calculated TGA curve. This was particularly true when the char yield was added by 30%; then the experimental TGA curve was 8.1% higher than the calculated TGA curve. Therefore, a chemical reaction occurred between the organic and inorganic phases during combustion. This can contribute to the formation of char and improve thermal stability and flame retardancy of the composites.

TGA

The thermal stability of pure epoxy and epoxy/bagasse@TGIC@DOPO IPN composites was investigated through thermogravimetric analysis. In a nitrogen environment, the temperature ranges from 30 to 800 °C. A TGA curve was used to indicate thermal stability, and a differential TGA analysis curve was used to observe the temperature of the maximum degradation rate [26].

The thermal analysis curve of composite materials introduced the epoxy to different amounts of flame retardants, as shown in Figs. 3 and 4. Relevant thermal degradation data such as the temperature of 10% mass loss (T_{d10}), temperature of the maximum thermal degradation rate (T_{max}), the maximum thermal degradation rate (R_{max}), and the char yield are listed in Table 2 [5].

Figures 3 and 4 and Table 2 indicate that regardless of the amount of epoxy/bagasse@TGIC@DOPO IPN composite materials added, the temperature of 10% mass loss was advanced. Bond breaking is more likely to occur in these materials than the C–C bond in pure epoxy and the P–C and O=P–O bonds in epoxy/bagasse@TGIC@DOPO IPN composite materials [27]. Therefore, the T_{d10} of pure epoxy was 400 °C, and when the addition was 30%, T_{d10} was reduced to 314 °C. Epoxy/bagasse@TGIC@DOPO IPN composite materials effectively reduced the maximum degradation rate of pure epoxy from − 33.4 to − 9.8 mass% min^{-1}, and increased the char yield from 14.1 to 23.4 mass% because the phosphorus in the bagasse@TGIC@DOPO structure traps free radicals in the gas phase and enters the condensed phase during the thermal degradation process. In addition, the phosphorus catalyzes char formation and the nitrogen in the structure, which releases noncombustible gas during the thermal degradation process and prompts the expansion of the char layer to prevent the fire from spreading [28]. The benzene ring generated char; thus, the char layer had antioxidation resistance to high-temperature combustion. The curve indicated considerable differences between these and indicated that adding phosphorus could improve the thermal stability of the composites during the high-temperature period.

Thermogravimetric analysis with infrared spectroscopy (TG-IR)

To investigate whether new toxic compounds are produced during thermal degradation, we conducted experiments

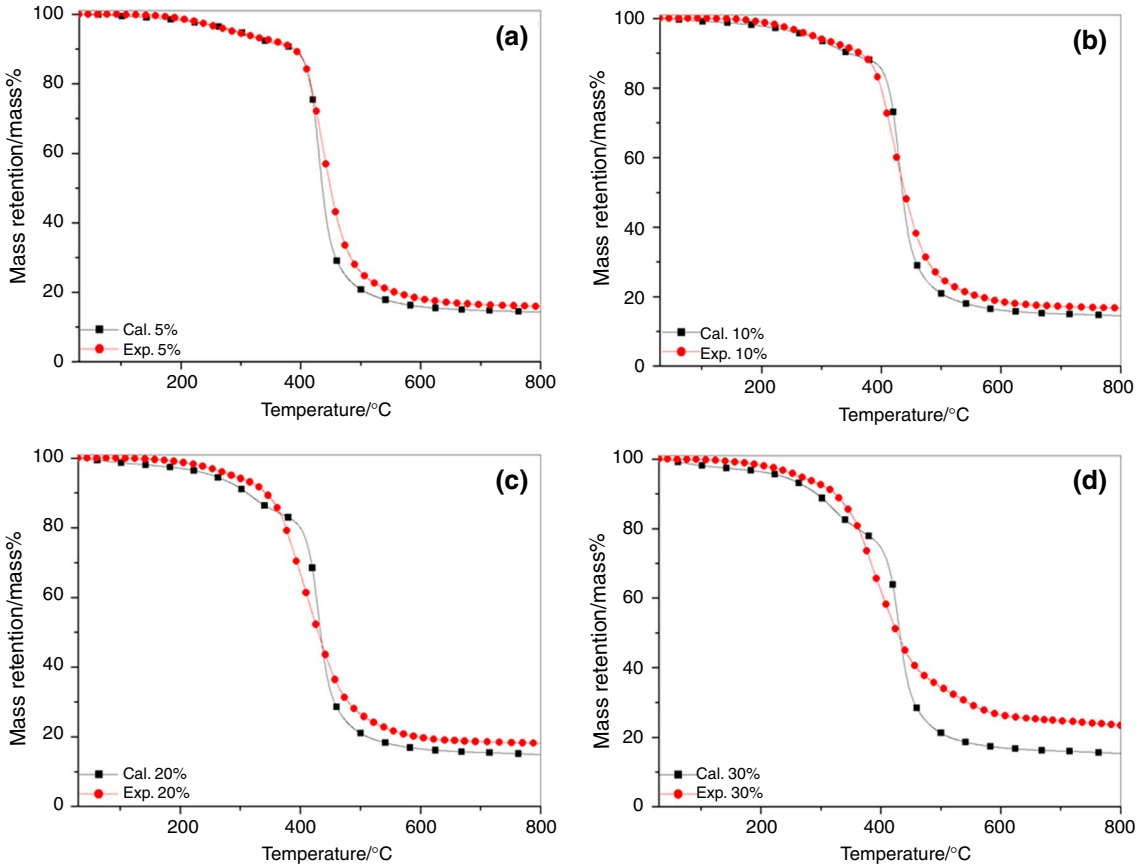

Fig. 2 Comparison of experimental and calculated TGA curves for **a** epoxy/bagasse@TGIC@DOPO IPN 5%, **b** epoxy/bagasse@TGIC@DOPO IPN 10%, **c** epoxy/bagasse@TGIC@DOPO IPN 20%, **d** epoxy/bagasse@TGIC@DOPO IPN 30% composites

Table 1 Comparison of calculated and experimental TGA data of epoxy/bagasse@TGIC@DOPO IPN 5–30% composites

Sample no	C.Y (mass%) at 800 °C	
	Cal	Exp
Epoxy/bagasse@TGIC@DOPO IPN 5%	14.3	15.9
Epoxy/bagasse@TGIC@DOPO IPN 10%	14.5	16.7
Epoxy/bagasse@TGIC@DOPO IPN 20%	14.9	18.1
Epoxy/bagasse@TGIC@DOPO IPN 30%	15.3	23.4

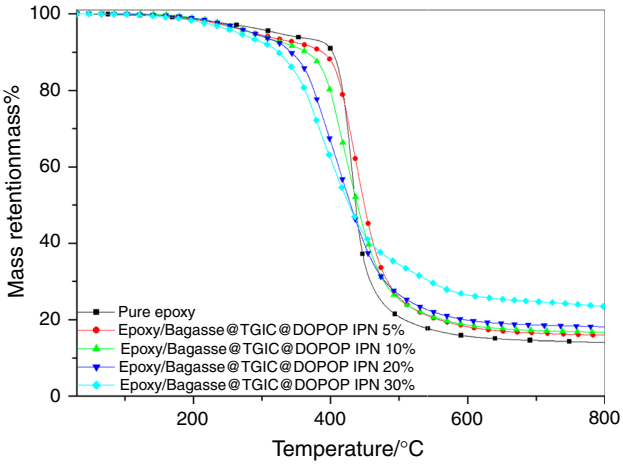

Fig. 3 TGA curves of epoxy and epoxy/bagasse@TGIC@DOPO IPN composites in N_2

under an air environment with a heating rate of 10 °C min^{-1} [29]. We used pure epoxy and epoxy/bagasse@TGIC@DOPO IPN with 30% composite materials to compare three-dimensional (3D) Fourier-transform infrared spectroscopy (FT-IR), as illustrated in Figs. 5 and 6, through thermogravimetric analysis with infrared spectroscopy (TG-IR). Characteristic absorption peaks at 2400–2250 and 586–726 cm^{-1} and absorption peaks of CO_2 at 1900–1650 cm^{-1} indicated aldehydes, ketones, and acids [30]. The CO_2 and aldehydes, ketones, and acid emission of pure epoxy were higher than those of epoxy/DOPO–TGIC–bagasse IPN with 30% composite materials. When a fire occurs, considerable acid damages human organs. Figures 7 and 8

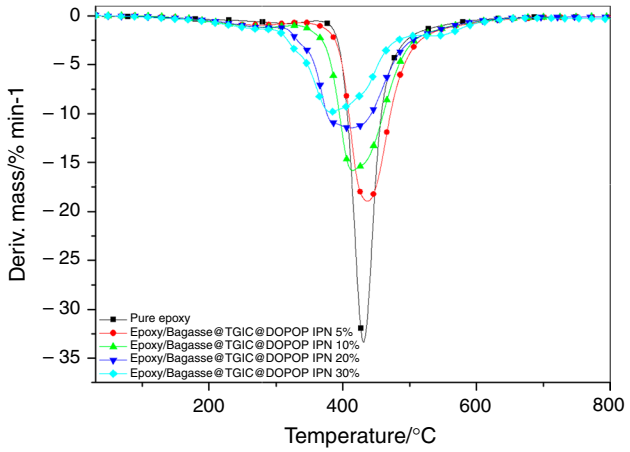

Fig. 4 Derivative curves of pure epoxy and epoxy/bagasse@TGIC@DOPO IPN composites in N_2

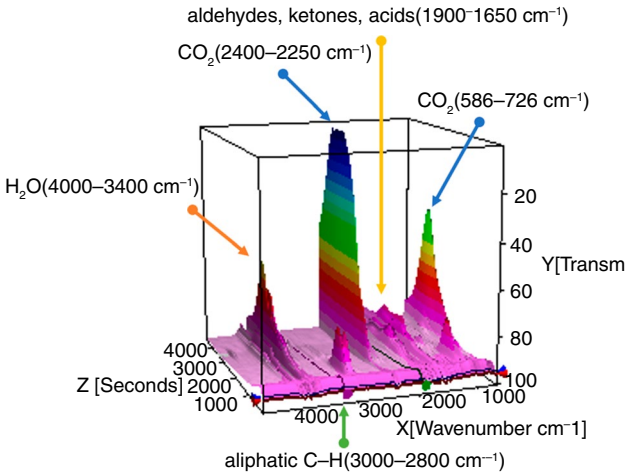

Fig. 5. 3D TG-IR spectrum of pure epoxy

illustrated that the characteristic absorption peaks of thermal degradation products were 2400–2250 cm^{-1} for CO_2, 2250–2000 cm^{-1} for CO, 1900–1650 cm^{-1} for aldehydes and anhydrides, 1690–1450 cm^{-1} for aromatic compounds, and 726–586 cm^{-1} for CO_2. Selecting a few representative temperatures (300–700 °C) [30] can elucidate the detailed thermal degradation processes of pure epoxy and epoxy/bagasse@TGIC@DOPO IPN with 30% composite materials. Figures 7 and 8 have one additional P=O (1250 cm^{-1}) [31]. Because of this functional group in the composite structure, phosphorus-containing parts began to degrade at low temperatures and prompt char production. As the temperature rose, pure epoxy released CO beginning at 300 °C. Compared with epoxy/bagasse@TGIC@DOPO IPN with 30% composite materials, the composite at 400 °C gradually released CO possibly because of the carbon layer protecting underlying material from further combustion caused by uncombusted materials [31]. The maximum degradation temperature of 600 °C in Fig. 9 revealed that the release amount of the pyrolysis gas product of epoxy/bagasse@TGIC@DOPO IPN with 30% composite materials was lower than that of pure epoxy because bagasse@TGIC@DOPO flame retardants have phosphorus and nitrogen-containing

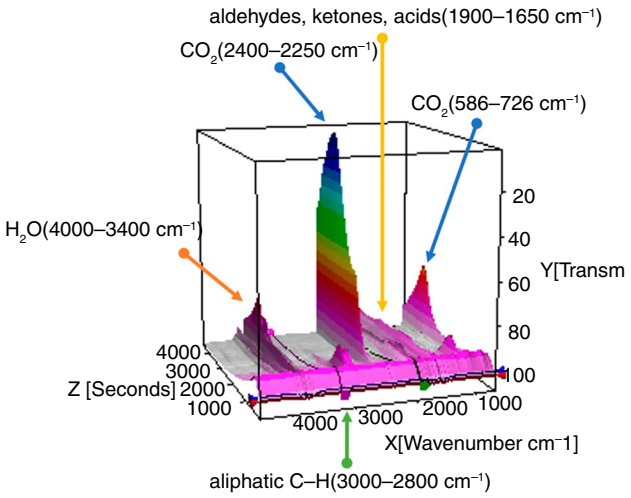

Fig. 6. 3D TG-IR spectrum of epoxy/bagasse@TGIC@DOPO IPN composites

Table 2 Thermal properties of epoxy and epoxy/bagasse@TGIC@DOPO IPN composites

Sample no	[a]T_{d10}/°C	[b]T_{max}/°C	[c]R_{max}/mass% min^{-1}	IPDT/°C	C.Y/mass%
Pure epoxy	400	430	−33.4	619	14.1
Epoxy/bagasse@TGIC@DOPO IPN 5%	378	436	−18.9	670	15.9
Epoxy/bagasse@TGIC@DOPO IPN 10%	354	414	−15.8	677	16.7
Epoxy/bagasse@TGIC@DOPO IPN 20%	336	410	−11.5	702	18.1
Epoxy/bagasse@TGIC@DOPO IPN 30%	314	382	−9.8	799	23.4

[a]T_{d10} is the temperature when the mass loss of the sample reaches its 10%

[b]T_{max} corresponds to the maximum temperature degradation rate

[c]R_{max} corresponds to the maximum thermal degradation rate

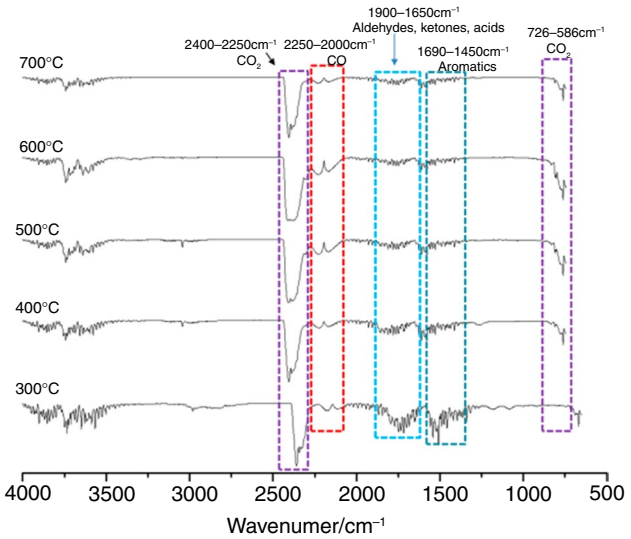

Fig. 7 FTIR identification of pure epoxy thermal degradation at the heating rate of 10 °C min^{-1} in air atmosphere

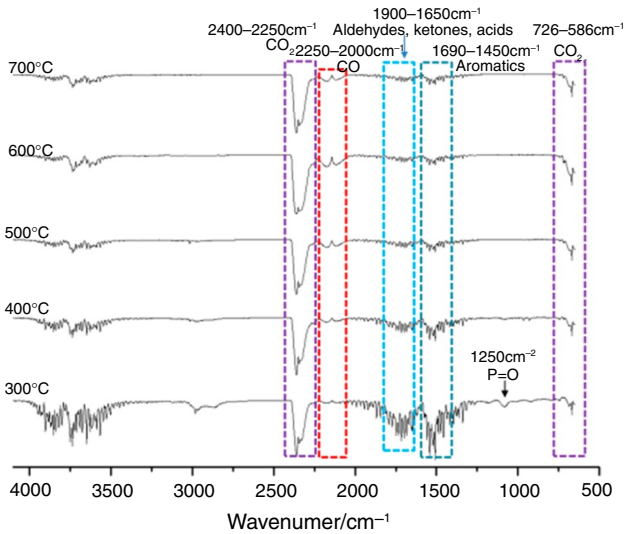

Fig. 8 FTIR identification of epoxy/bagasse@TGIC@DOPO IPN composites during thermal degradation at the heating rate of 10 °C min^{-1} in air atmosphere

elements that can capture free radicals and release incombustible gases [28], thereby increasing the thermal stability and fire safety of pure epoxy.

LOI UL-94

The UL-94 uses a burning standard test piece to record whether the total burning time of two burnings pass the standard and observe whether cotton laid under a flame is ignited by dripping and melting to determine the

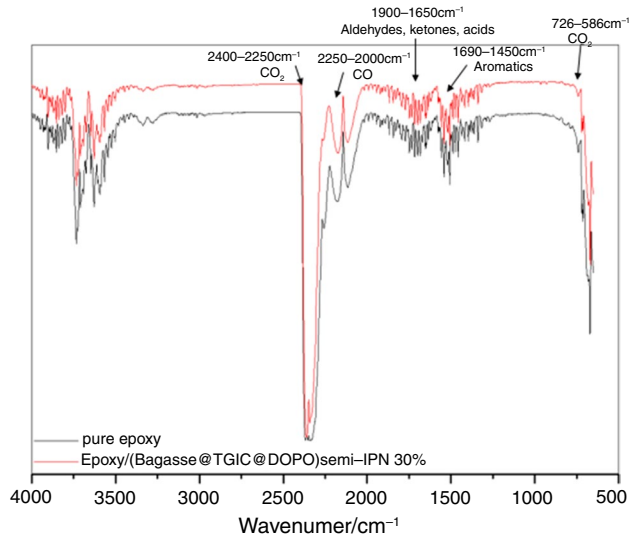

Fig. 9 TG-FTIR spectra of pure epoxy and epoxy/bagasse@TGIC@DOPO IPN 30% at maximum decomposition rates

flame-retardant level of polymer materials and categorize them into three levels: V-0, V-1, and V-2. The limiting oxygen index (LOI) determines the flame-retardant level of polymer materials by oxygen and nitrogen concentrations. The oxygen content of the atmosphere is 21%, and materials with an LOI of 21% or less burn in the air. Materials with an LOI of 22–25% automatically extinguish when burned, and materials with an LOI of at least 26% are difficult to ignite [32]. The flow rate of the adjusted oxygen and nitrogen was set to (mL/s), and its formula is as follows:

$$\mathrm{LOI} = \frac{O_2}{O_2 + N_2} \times 100$$

Table 3 shows that the LOI of epoxy was 21% and thus is a flammable polymer material. When the flame-retardant concentration was increased to 30%, the concentration of epoxy/bagasse@TGIC@DOPO IPN composite material increased to 29%, which indicated that flame retardance increased by eight levels. Epoxy failed the UL-94 and underwent violent burning as the added concentration increased to 30%. The flame burning time of the bagasse@TGIC@DOPO IPN composite materials was 1.6 and 1.2 s, respectively, before being extinguished; thus they are V-0 level. Therefore, the bagasse@TGIC@DOPO flame retardant has an excellent flame-retardant effect because the phosphorus in its structure traps free radicals during the gas phase and enters the condensed phase during thermal cracking; in addition, it catalyzes the formation of char and the nitrogen in the structure, which releases noncombustible gas during the thermal degradation process and prompts the expansion of the char layer to prevent the fire from spreading [31].

Table 3 The flame retardance of epoxy/bagasse@TGIC@DOPO IPN composites by LOI and UL-94

Sample	UL-94				LOI/%	ΔLOI/%	P-content/mass%	[b]EFF
	t1/s	t2/s	Ranking	Dripping				
Pure epoxy	[a]BC	–	Fail	No	21	0	0	0
Epoxy/bagasse@TGIC@DOPO IPN 5%	12.3 ± 0.5	BC	Fail	No	25	4	0.3	13.3
Epoxy/bagasse@TGIC@DOPO IPN 10%	10.5 ± 0.4	BC	Fail	No	27	6	0.6	10.0
Epoxy/bagasse@TGIC@DOPO IPN 20%	5.8 ± 0.3	BC	Fail	No	28	7	1.3	5.4
Epoxy/bagasse@TGIC@DOPO IPN 30%	1.6 ± 0.1	1.2 ± 0.1	V0	No	29	8	1.9	4.2
Epoxy/TGIC-DOPO 30%	0.7 ± 0.1	5.8 ± 0.2	V-0	No	26	6	2.1	2.88

[a]BC burn to the clamp

[b]EFF = ΔLOI/P-content (mass%)

The benzene ring contributes to the amount of char produced; thus, the char layer can prevent high-temperature combustion.

In addition, Table 3 indicates that as bagasse@TGIC@DOPO increases, effective flame retardancy increased. Subsequently, as the addition increased to the maximum value, effective flame retardance reduced. Although bagasse@TGIC@DOPO with a 30% LOI value reached flame retardancy, bagasse@TGIC@DOPO with a 5% LOI value had excellent effective flame retardance. This suggested that bagasse@TGIC@DOPO with a 5% LOI value had excellent flame-retardant efficiency for composite materials [33, 34]. We have compared the flame-retardant property of the composites without bagasse. We found out that bagasse is helpful for retardant property in the same mass percentage of the additives in Table 3.

EDS

During energy-dispersive X-ray spectroscopy (EDS), an electron beam produces the characteristic X-ray of a sample element when it hits the sample. This can be used to analyze the composition of surface materials to determine their main components and use quantitative and elemental distribution diagrams to discuss epoxy/bagasse@TGIC@DOPO IPN with 5% and 30% element changes before and after combustion. Figure 10 illustrates elemental changes in epoxy/bagasse@TGIC@DOPO IPN with 5% and 30% element changes before burning. Figure 10a indicates that epoxy/bagasse@TGIC@DOPO IPN with 5% element change contained three elements—C, O, and P—and the percentages of their mass were 73.72%, 25.72%, and 0.56%, respectively. Figure 10b illustrates that the epoxy/bagasse@TGIC@DOPO IPN with 30% element change had three types of elements, C, O, and P, and the percentages of their mass were 72.79%, 24.95%, and 2.26%. As the addition amount increased, the phosphorus content increased. Figure 10c shows that epoxy/bagasse@TGIC@DOPO IPN with 30% element change had three types of elements, C, O, and P, after burning, and the percentages of their mass were 67.54%, 20.97%, and 11.49%, respectively. During burning, char was formed because of the dehydration of phosphorus elements. In addition, nitrogen released noncombustible gas during combustion and prompted the expansion of the char

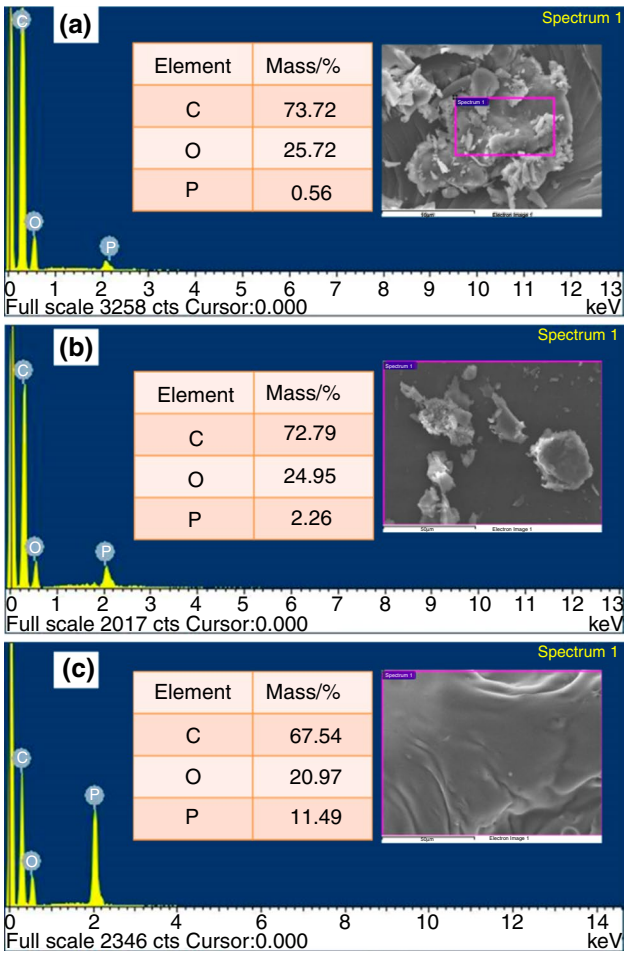

Fig. 10 EDS of **a** epoxy/bagasse@TGIC@DOPO IPN 5% before burning, **b** epoxy/bagasse@TGIC@DOPO IPN 30% before burning, **c** epoxy/bagasse@TGIC@DOPO IPN 30% after burning

layer to prevent the fire from spreading [31]. The benzene ring supported the amount of char produced and can thus prevent passage between the gas and ignition source.

X-ray photoelectron spectroscopy analysis

X-ray photoelectron spectroscopy (XPS) was used to verify changes in chemical bonds produced by epoxy/bagasse@TGIC@DOPO IPN composite materials at room temperature and after burning at 800 °C by using a high-temperature furnace. We observed changes in the functional groups before and after combusting the flame retardant added to epoxy. Wave peak separation was used to calculate the antioxidation properties of composite materials, and the results are displayed in Figs. 11–16 and Tables 4 and 5.

The XPS rough scans in Figs. 11 and 12 present the element changes of epoxy/bagasse@TGIC@DOPO IPN with 5% element changes and that with 30% element chances at room temperature and at a high temperature of 800 °C. Figure 11a indicates that the elements appearing at room temperature were C, O, N, P, and Si. Figure 11b shows that the elements appearing at a temperature of 800 °C and at room temperature were the same. Following a deep oxidation at 800 °C in the high-temperature furnace, the amount of C and P increased. During the thermal degradation process of DOPO, phosphoric acid can be produced as a dehydrating agent and promote the formation of char [35], thereby protecting it from high-temperature attacks of the epoxy resin substrate.

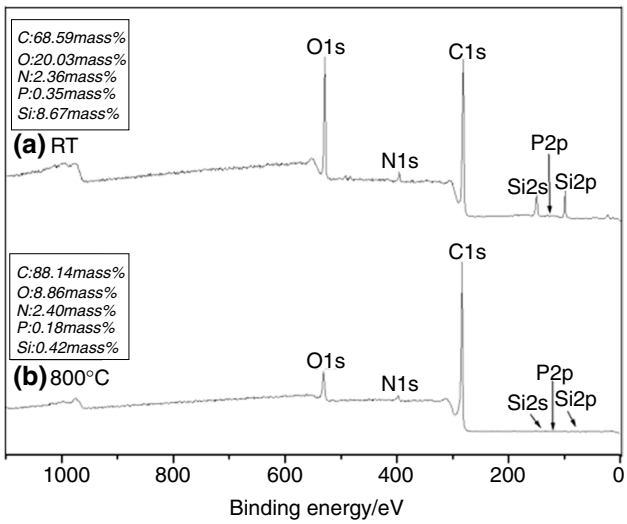

Fig. 11 XPS spectra of epoxy/bagasse@TGIC@DOPO IPN 5% **a** RT, **b** 800 °C

Table 5 The values of Cox/Ca of composites at RT and 800 °C

Sample no	Temperature	
	RT	800 °C
Epoxy/bagasse@TGIC@DOPO IPN 5%	0.18	0.15
Epoxy/bagasse@TGIC@DOPO PN 30%	0.16	0.09

Figures 13–16 display changes in the types of bonding of the fine scan spectra of Cls, Ols, and Si2p at room temperature and at a high temperature of 800 °C.

First, the Cls spectrum contains a total of six functional groups located at 284 eV (C–C/C–H) [36], 285.4 eV (C–N) [37], C=C 284.5 eV [38], 286 eV (C–O) [39], and 282.9 eV (C–Si) [40], respectively. Following thermal oxidation at a high temperature of 800 °C, the C=O structure at 288.9 eV occurred [41]. The material structure was mainly graphitized after high-temperature combustion and thus the C=C structure improved. The results are illustrated in Figs. 13 and 14.

The Ols spectrum contains a total of three types of functional groups located at 531.2 eV (=O) [42], 533 eV (–O) [43], and 531.5 eV (P=O) [44], respectively. This explains the changing bond types under room temperature and high-temperature thermal oxidation because the DOPO of the flame retardant has a functional group of P=O. The phosphorus element was dehydrated to form char, and the nitrogen element released noncombustible gas during combustion, thereby prompting the expansion of the char layer to prevent the fire from spreading [28]. After high-temperature thermal oxidation, P=O increased significantly, and the results are shown in Fig. 15.

Table 4 Binding energy (eV) and relative peak intensities (%) of the various components of C1s peak-fitted signals

Sample no	C1s					
	C–C/C–H	C=C	C–N	C–Si	C–O	C=O
Epoxy/bagasse@TGIC@DOPO IPN 5%-RT	0.38 ± 0.02	0.29 ± 0.01	0.04 ± 0.01	0.14 ± 0.01	0.15 ± 0.01	–
Epoxy/bagasse@TGIC@DOPO IPN 5%-800 °C	0.24 ± 0.01	0.33 ± 0,02	0.13 ± 0.01	0.16 ± 0.01	0.07 ± 0.01	0.06 ± 0.01
Epoxy/bagasse@TGIC@DOPO IPN 30%-RT	0.42 ± 0.01	0.21 ± 0.01	0.06 ± 0.01	0.17 ± 0.01	0.14 ± 0.01	–
Epoxy/bagasse@TGIC@DOPO IPN 30%-800 °C	0.31 ± 0.01	0.19 ± 0.01	0.17 ± 0.01	0.24 ± 0.01	0.04 ± 0.01	0.04 ± 0.01

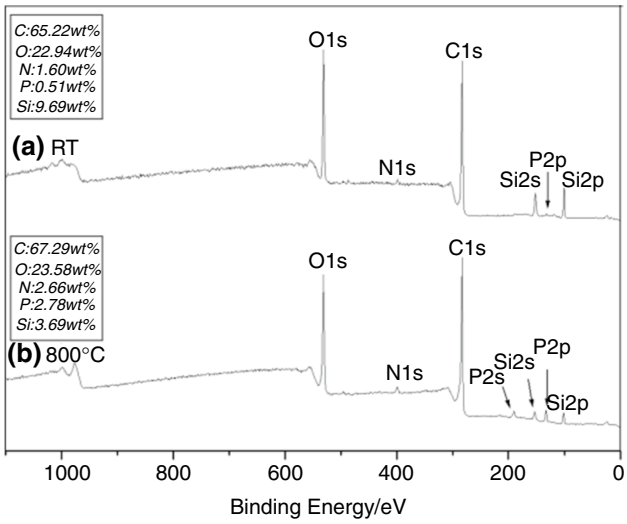

Fig. 12 XPS spectra of epoxy/bagasse@TGIC@DOPO IPN 30% **a** RT, **b** 800 °C

In the Si2p spectrum, Fig. 16a, b shows that bonding strength changed considerably before and after combustion, and Fig. 16a indicates that bagasse was added to the flame retardant; thus, bagasse contains a small amount of Si [45, 46]. Two types of bonding were identified: 100.7 eV (Si–C) [47] and 103.6 eV (SiO_2) [48]. Figure 16b indicates that the following oxidation with combustion heat caused the silicide to be converted to silicon dioxide; thus, the SiO_2 peak intensity increased. Therefore, epoxy/bagasse@TGIC@DOPO IPN composite materials produce a car layer after burning to protect the substrate.

We analyzed the difference between oxidation epoxy/bagasse@TGIC@DOPO IPN at 5% and that at 30% before and after combustion thermal oxidation. After using the Cls spectrum to calculate the area ratio of each bond species individually, the antioxidant effect of the material was obtained through oxidized carbons (Cox)/aliphatic aromatic carbons (Ca) [49]. The results are presented in Figs. 13 and 14 and Tables 4 and 5. Table 5 indicates that after adding 5% and 30% concentration of the composite material, the ratio of Cox/Ca at room temperature was 0.18 and 0.16, respectively. After burning at a high temperature, the ratio dropped to 0.15 and 0.09, respectively. In summary, a high concentration of the addition resulted in superior resistance to oxidation and improved the thermal stability of hybrid materials.

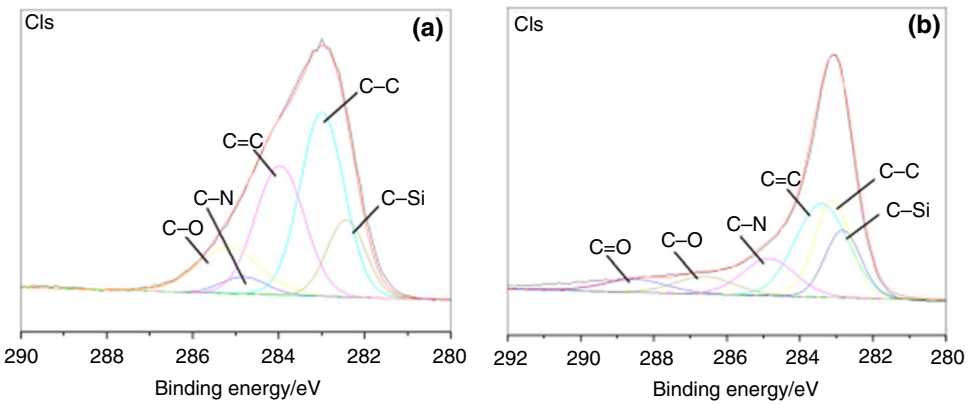

Fig. 13 C1s spectra of epoxy/bagasse@TGIC@DOPO IPN 5% **a** RT, **b** under air atmosphere at 800 °C

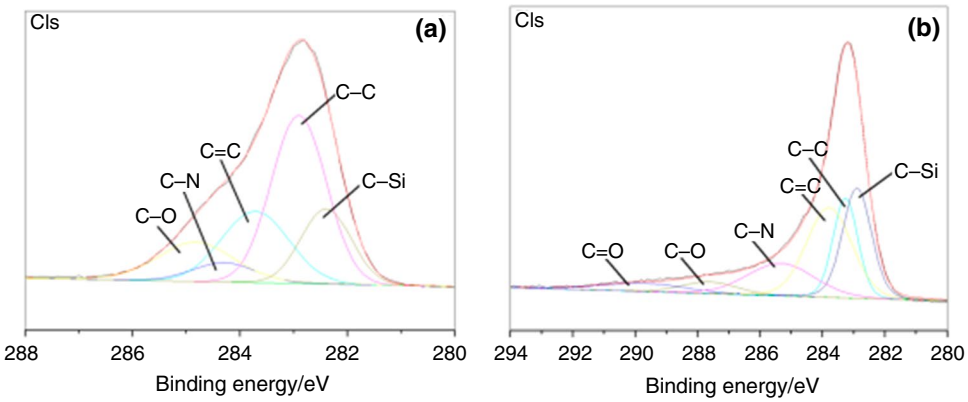

Fig. 14 C1s spectra of epoxy/bagasse@TGIC@DOPO IPN 30% **a** RT, **b** under air atmosphere at 800 °C

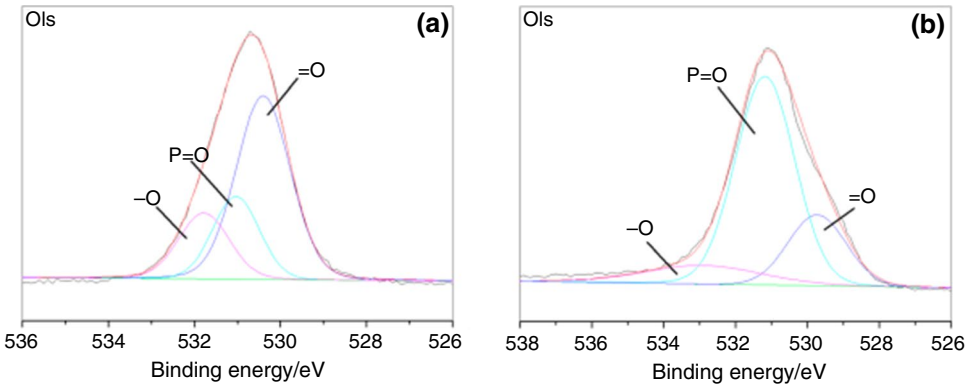

Fig. 15 O1s spectra of epoxy/bagasse@TGIC@DOPO IPN 30% **a** RT, **b** under air atmosphere at 800 °C

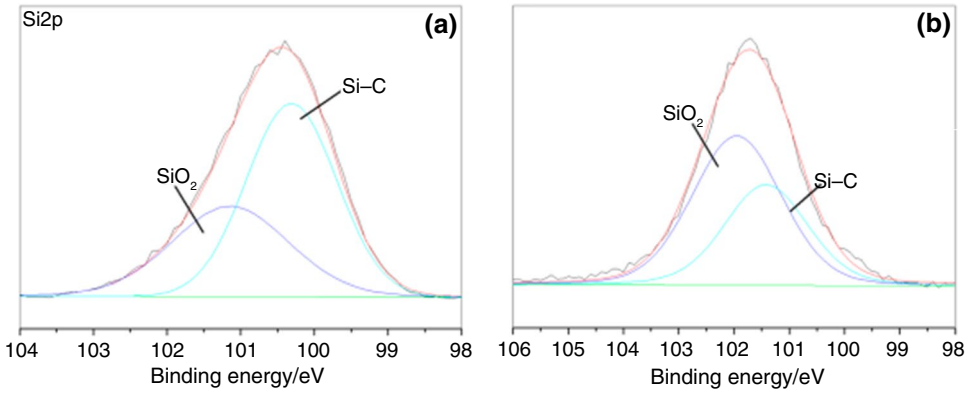

Fig. 16 Si2p spectra of epoxy/bagasse@TGIC@DOPO IPN 30% **a** RT, **b** under air atmosphere at 800 °C

Conclusions

This study successfully synthesized flame retardant a bagasse@TGIC@DOPO and included it into the epoxy resin substrate to prepare effective flame-retardant epoxy/bagasse@TGIC@DOPO IPN composite materials. Compared with pure epoxy, the addition of bagasse@TGIC@DOPO increased thermal stability, flame retardancy, and oxidation resistance of the composite material. When the flame retardant was added to 30% composite materials, the char rate was 23.4 mass%, which was 9.3 mass% higher than that of pure epoxy (14.1 mass%). The LOI and UL-94 also increased from 21 (fail) to 29 (V-0). The results revealed that the flame retardant we added to the substrate had a noticeable fire protection effect. The use of epoxy in transportation, coating materials, composite materials, and construction materials can reduce the chance of fire.

Acknowledgments The authors would like to express their appreciation to the National Science Council of the Republic of China for financial support of this study under Grant MOST-108-2221-E-241-007 & MOST 107-2221-E-167-030-MY2

References

1. Jian RK, Ai YF, Xia L, Zhao LJ, Zhao HB. Single component phosphamide-based intumescent flame retardant with potential reactivity towards low flammability and smoke epoxy resins. J Hazard Mater. 2019;371:529–39.
2. Luo Q, Sun Y, Yu B, Li C, Song J, Tan D, Zhao J. Synthesis of a novel reactive type flame retardant composed of phenophosphazine ring and maleimide for epoxy resin. Polym Degrad Stab. 2019a;165:137–44.
3. Huo S, Liu Z, Li C, Wang X, Cai H, Wang J. Synthesis of a phosphaphenanthrene/benzimidazole-based curing agent and its application in flame-retardant epoxy resin. Polym Degrad Stab. 2019;163:100–9.
4. Chen R, Hu K, Tang H, Wang J, Zhu F, Zhou H. A novel flame retardant derived from DOPO and piperazine and its application in epoxy resin: Flame retardance, thermal stability and pyrolysis behavior. Polym Degrad Stab. 2019;166:334–43.
5. Wang P, Chen L, Xiao H. Flame retardant effect and mechanism of a novel DOPO based tetrazole derivative on epoxy resin. J Anal Appl Pyrolysis. 2019;139:104–13.
6. Zhu ZM, Wang LX, Dong LP. Influence of a novel P/N-containing oligomer on flame retardancy and thermal degradation of intumescent flame-retardant epoxy resin. Polym Degrad Stab. 2019;162:129–37.
7. Chen X, Ma C, Jiao C. Enhancement of flame-retardant performance of thermoplastic polyurethane with the incorporation of aluminum hypophosphite and iron-graphene. Polym Degrad Stab. 2016;129:275–85.
8. Mark J, Guardia L, Hale RC. Halogenated flame-retardant concentrations in settled dust, respirable and inhalable particulates and polyurethane foam at gymnastic training facilities and residences. Environ Int. 2015;79:106–14.
9. Directive 2012/19/EU of the European parliament and of the council of 4 July 2012 on waste electrical and electronic equipment (WEEE). Off J Eur Union. 2012;197:38

10. Directive 2011/65/EU of the European parliament and of the council of 8 June 2011 on the restriction of the use of certain hazardous substances in electrical and electronic equipment. Off J Eur Union. 2011;174:88
11. Directive (EU) 2017/2102 of the European parliament and of the council of 15 November 2017 amending Directive 2011/65/EU on the restriction of the use of certain hazardous substances in electrical and electronic equipment. Off J Eur Union. 2017;305:8
12. Guna V, Ilangovan M, Hu C, Venkatesh K, Reddy N. Valorization of sugarcane bagasse by developing completely biodegradable composites for industrial applications. Ind Crop Prod. 2019;131:25–31.
13. Griffin GJ. The effect of fire retardants on combustion and pyrolysis of sugar-cane bagasse. Bioresour Technol. 2011;102:8199–204.
14. Maschio LJ, Pereira PHF, Silva MLCP. Preparation and characterization of cellulose/hydrous niobium oxide hybrid. Carbohydr Polym. 2012;89:992–6.
15. Jian R, Wang P, Duan W, Wang J, Zheng X, Weng J. Synthesis of a novel P/N/S-Containing flame retardant and its application in epoxy Resin: thermal property, flame retardance, and pyrolysis behavior. Ind Eng Chem Res. 2016;55(44):11520–7.
16. Luo Q, Sun Y, Yu B, Li C, Song J, Tan D, Zhao J. Synthesis of a novel DPPA-containing benzoxazine to flame-retard epoxy resin with maintained thermal properties. Polym Adv Technol. 2019b;30:1989–95.
17. Bousalem S, Zeggai FZ, Baltach H, Benyoucef A. Physical and electrochemical investigations on hybrid materials synthesized by polyaniline with various amounts of ZnO nanoparticle. Chem Phys Lett. 2020;741:137095.
18. Kusumoto T, Mori Y, Kanasaki M, Ueno T, Kameda Y, Oda K, Kodaira S, Kitamura H, Barillon R, Yamauchi T. Yields on the formation of OH groups and the loss of CH groups along nuclear tracks in PADC films. Radiat Meas. 2015;83:59–62.
19. Sritham E, Gunasekaran S. FTIR spectroscopic evaluation of sucrose-maltodextrin-sodium citrate bioglass. Food Hydrocoll. 2017;70:371–82.
20. Sideridou ID, Vouvoudi EC, Papadopoulos GD. Epoxy polymer Hxtal NYL-1TM used in restoration and conservation: irradiation with short and long wavelengths and study of photo-oxidation by FT-IR spectroscopy. J Cult Herit. 2016;18:279–89.
21. Bagherzadeh MR, Daneshvar A, Shariatpanahi H. Novel water-based nanosiloxane epoxy coating for corrosion protection of carbon steel. Surf Coat Technol. 2012;206(8–9):2057–63.
22. Zhang YC, Xu GL, Liang Y, Jin Y, Hu J. Preparation of flame retarded epoxy resins containing DOPO group. Thermochim Acta. 2016;643:33–40.
23. Yao Z, Ma X, Wu Z, Yao T. TGA–FTIR analysis of co-pyrolysis characteristics of hydrochar andpaper sludge. J Anal Appl Pyrolysis. 2017;123:40–8.
24. Mu L, Chen J, Yin H, Song X, Li A, Chi X. Pyrolysis behaviors and kinetics of refining and chemicals wastewater, lignite and their blends through TGA. Bioresour Technol. 2015;180:22–31.
25. Lin X, Kong L, Cai H, Zhang Q, Bi D, Yi W. Effects of alkali and alkaline earth metals on the co-pyrolysis of cellulose and high density polyethylene using TGA and Py-GC/MS. Fuel Process Technol. 2019;191:71–8.
26. Wei KK, Leng TP, Keat YC, Osman H, Rasidi MSM. The potential of natural rubber (NR) in controlling morphology in two matrix epoxy/NR/graphene nano-platelets (GNP) systems. Polym Test. 2019;77:105905.
27. Wang X, Zhou S, Guo WW, Wang PL, Xing WY, Song L, Hu Y. Renewable cardanol-based phosphate as a flame retardant toughening agent for epoxy resins. ACS Sustain Chem Eng. 2017;5:3409–16.
28. Velencoso MM, Ramos JM, Klein R, Lucas AD, Rodriguez FJ. Thermal degradation and fire behaviour of novel polyurethanes based on phosphate polyols. Polym Degrad Stab. 2014;101:40–51.
29. Lu Y, Jia Y, Zhou Y, Zou J, Zhang G, Zhang F. Straightforward one-step solvent-free synthesis of the flame retardant for cotton with excellent efficiency and durability. Carbohydr Polym. 2018;201:438–45.
30. Ding H, Huang K, Li S, Xu L, Xia J, Li M. Synthesis of a novel phosphorus and nitrogen-containing bio-based polyol and its application in flame retardant polyurethane foam. J Anal Appl Pyrolysis. 2017a;128:102–13.
31. Ma Z, Wang J, Yang Y, Zhang Y, Zhao C, Yu Y, Wang S. Comparison of the thermal degradation behaviors and kinetics of palm oil waste under nitrogen and air atmosphere in TGA-FTIR with a complementary use of model-free and model-fitting approaches. J Anal Appl Pyrolysis. 2018;134:12–24.
32. Yang R, Hu W, Xu L, Song Y, Li J. Synthesis, mechanical properties and fire behaviors of rigid polyurethane foam with a reactive flame retardant containing phosphazene and phosphate. Polym Degrad Stab. 2015;122:102–9.
33. Ding H, Huang K, Li S, Xu L, Xia J, Li M. Flame retardancy and thermal degradation of halogen-free flame retardant biobased polyurethane composites based on ammonium polyphosphate and aluminium hypophosphite. Polym Test. 2017b;62:325–34.
34. Feng C, Zhang Y, Liang D, Liu S, Chi Z, Xu J. Flame retardancy and thermal degradation behaviors of polypropylene composites with novel intumescent flame retardant and manganese dioxide. J Anal Appl Pyrolysis. 2013;104:59–67.
35. Xu MJ, Xu GR, Leng Y, Li B. Synthesis of a novel flame retardant based on cyclotriphosphazene and DOPO groups and its application in epoxy resins. Polym Degrad Stab. 2016;123:105–14.
36. Liu W, Chen DQ, Wang YZ, Wang DY, Qu MH. Char-forming mechanism of a novel polymeric flame retardant with char agent. Polym Degrad Stab. 2007;92:1046–52.
37. Chen X, Hu Y, Jiao C, Song L. Preparation and thermal properties of a novel flame-retardant coating. Polym Degrad Stab. 2007;92:1141–50.
38. Teng CC, Ma CCM, Lu CH, Yang SY, Lee SH, Hsiao MC, Yen MY, Chiou KC, Lee TM. Thermal conductivity and structure of non-covalent functionalized graphene/epoxy composites. Carbon. 2011;49(15):5107–16.
39. Zhou S, Song L, Wang Z, Hu Y, Xing W. Flame retardation and char formation mechanism of intumescent flame retarded polypropylene composites containing melamine phosphate and pentaerythritol phosphate. Polym Degrad Stab. 2008;93:1799–806.
40. Wang Z, Wei P, Qian Y, Liu J. The synthesis of a novel graphene-based inorganic–organic hybrid flame retardant and its application in epoxy resin. Compos Part B-Eng. 2014;60:341–9.
41. Xu B, Wu X, Ma W, Qian L, Xin F, Qiu Y. Synthesis and characterization of a novel organic-inorganic hybrid char forming agent and its flame-retardant application in polypropylene composites. J Anal Appl Pyrolysis. 2018;134:231–42.
42. Dutkiewicz M, Przybylak M, Januszewski R, Maciejewski H. Synthesis and flame retardant efficacy of hexakis (3-(triethoxysilyl) propyloxy)cyclotriphosphazene/silica coatings for cotton fabrics. Polym Degrad Stab. 2018;148:10–8.
43. Shi Y, Belosinschi D, Brouillette F, Belfkira A, Chabot B. Phosphorylation of Kraft fibers with phosphate esters. Carbohydr Polym. 2014;106:121–7.
44. Kannan GA, Choudhury NR, Dutta KN. Synthesis and characterization of methacrylate phospho-silicate hybrid for thin film applications. Polymer. 2007;48(24):7078–86.
45. Lizet RM, Luis EAP, Raúl APB, Yannay CLWP, Frederik R. Effect of citric acid leaching on the demineralization and thermal degradation behavior of sugarcane trash and bagasse. Biomass Bioenerg. 2018;108:371–80.

46. Janbuala S, Eambua M, Satayavibul A, Nethan W. Effect of bagasse and bagasse ash levels on properties of pottery products. Heliyon. 2018;4(9):e00814.
47. Brookes NP, Fraser S, Short DR, Hanley L, Fuoco E, Roberts A, Hutton S. The effect of ion energy on the chemistry of air-aged polymer films grown from the hyperthermal polyatomic ion Si_2OMe^{5+}. J Electron Spectrosc Relat Phenom. 2001;121:281–97.
48. Kim CY, Kim SH, Navamathavan R, Choi CK, Jeung WY. Characteristics of low-k SiOC(–H) films deposited at various substrate temperature by PECVD using DMDMS/O_2 precursor. Thin Solid Films. 2007;516:340–4.
49. Wang X, Wu L, Li J. Synergistic flame retarded poly(methyl methacrylate) by nano-ZrO_2 and triphenylphosphate. J Therm Anal Calorim. 2011;10:741–6.